Applied Mathematics and Statistics
https://www.sciltp.com/journals/ams

Article

An Adaptive Residual-Controlled Overlapping Taylor Method for Nonlinear Duffing, Van der Pol, and Mathieu-Type Oscillators

Mehmet Çevik [1,*], Sümeyye Sınır [2] and Nurcan Baykuş Savaşaneril [3]

[1] Department of Mechanical Engineering, İzmir Katip Çelebi University, 35620 İzmir, Türkiye
[2] General Coordination Office of Projects, İzmir Katip Çelebi University, 35620 İzmir, Türkiye
[3] İzmir Vocational School, Dokuz Eylül University, 35380 İzmir, Türkiye
* Correspondence: mehmet.cevik@ikcu.edu.tr

How To Cite: Çevik, M.; Sınır, S.; Savaşaneril, N.B. An Adaptive Residual-Controlled Overlapping Taylor Method for Nonlinear Duffing, Van der Pol, and Mathieu-Type Oscillators. *Applied Mathematics and Statistics* **2026**, *3*(2), 17. https://doi.org/10.53941/ams.2026.100017

Received: 22 July 2026
Revised: 14 August 2026
Accepted: 20 August 2026
Published: 25 August 2026

Abstract: This study presents a new adaptive high-order numerical framework, called the Adaptive Residual-Controlled Overlapping Taylor (ARCOT) method, for the solution of strongly nonlinear oscillatory systems. The proposed approach combines high-order local Taylor expansion, overlapping continuation intervals, residual-controlled adaptivity, and adaptive continuation interval regulation within a unified computational framework. Unlike conventional Taylor continuation methods based on fixed interval propagation, ARCOT continuously monitors the governing equation residual and dynamically adjusts continuation intervals according to the local nonlinear behavior of the solution. Overlapping continuation points are additionally employed to improve long-time numerical stability and suppress cumulative propagation errors. The effectiveness of the proposed methodology is investigated through several benchmark nonlinear oscillators, including Duffing, cubic–quintic, nonlinear Van der Pol, Mathieu-type, and double-well systems. Numerical results obtained using ARCOT are compared with RK4, adaptive RK45, Taylor-based approaches, and available analytical or semi-analytical solutions reported in the literature. The obtained results demonstrate that ARCOT provides highly accurate displacement responses, stable phase-plane trajectories, and reliable long-time integration behavior without noticeable numerical drift. Residual evolution and adaptive continuation histories further confirm that the proposed residual-control mechanism effectively regulates local approximation quality while automatically adapting continuation intervals according to nonlinear response characteristics. The numerical investigations indicate that ARCOT provides a robust, accurate, and flexible computational framework for nonlinear oscillatory systems with considerable extension potential toward fractional, delay, chaotic, and distributed dynamical systems.

Keywords: nonlinear oscillators; Taylor series methods; adaptive continuation; residual-controlled methods; DVdP oscillator; Mathieu equation

1. Introduction

Differential equations are among the most essential mathematical tools for describing the behavior of physical, engineering, biological, and computational systems. Ordinary differential equations (ODEs), partial differential equations (PDEs), fractional differential equations, delay differential equations, and integro-differential equations are widely used to model vibration, structural dynamics, wave propagation, heat transfer, diffusion, viscoelasticity, electromechanical systems, fluid mechanics, population dynamics, and control systems. In mechanical and structural engineering, single-degree-of-freedom (SDOF) systems provide a fundamental framework for understanding more complex dynamical systems. Linear and nonlinear oscillators such as Duffing, Van der Pol, Mathieu, cubic–quintic, and delayed vibration models have therefore attracted continuous attention in both theoretical and applied research. Because exact analytical solutions are generally unavailable for strongly nonlinear, time-dependent, fractional, or delayed systems, reliable approximate and numerical methods remain indispensable.

A wide range of methods has been developed for solving differential equations and nonlinear vibration problems. Classical approaches include Runge–Kutta methods, finite difference methods, finite element methods, collocation techniques, perturbation methods, harmonic balance, multiple scales, decomposition methods, homotopy perturbation methods, variational formulations, and neural-network-based methods. For mechanical systems, Samaniego et al. [1] emphasized the relevance of deep neural networks as approximation tools for computational mechanics, while Bulut and Yiğider [2] applied physics-informed neural networks to beta-conformable fractional differential equations. Similarly, Ali et al. [3] proposed Hermite wavelet neural network formulations for fractional PDEs, and Abdellatif et al. [4] used artificial neural networks to predict the maximum response of SDOF systems. These studies indicate the growing importance of data-driven and physics-informed solution strategies. In vibration analysis, Kim [5] developed a variational temporal finite element approach for nonlinear damping systems, whereas Chen et al. [6] investigated nonlinear SDOF systems in rod-coupling vibration control. Bayat and Pakar [7] introduced a modified Variational Approach to derive highly accurate analytical solutions for nonlinear oscillation systems. Boone et al. [8] studied model validation for nonlinear SDOF oscillators, and Witkowski et al. [9] analyzed experimentally motivated Duffing-type systems with double-well potentials. Fundamental and application-oriented SDOF studies have also been reported by Fujii et al. [10], Salsa Junior [11], Newaz et al. [12], McIntosh et al. [13], and Kojima and Takewaki [14], demonstrating the continuing importance of SDOF models in vibration theory, swept-sine response, free vibration, energy input, and earthquake-type dynamic loading.

Nonlinear oscillators have been investigated using both analytical and numerical tools. Neal and Nayfeh [15] examined nonlinear SDOF systems under subharmonic and nonstationary parametric excitations using multiple scales. Mehdipour et al. [16] applied the Energy Balance Method to obtain approximate analytical solutions for four different nonlinear differential equations governing vibrations and oscillations. Zavodney et al. [17] studied quadratic and cubic nonlinearities under principal parametric resonance and reported complex dynamic responses including bifurcations and chaotic behavior. Alevras and Yurchenko [18] analyzed nonlinear Mathieu-type parametric excitation in a pendulum system, while Kural [19] applied multiple scales to nonlinear axially moving strings with spring-loaded supports. Beléndez et al. [20] obtained exact solutions for cubic–quintic Duffing oscillators in terms of elliptic functions, and Vakakis and Blanchard [21] presented exact steady-state solutions for strongly nonlinear Duffing oscillators under special time-periodic excitations. More recently, Moatimid and Amer [22] investigated the stability of a ϕ6-Van der Pol oscillator, and Salas et al. [23] analyzed Duffing–Van der Pol oscillators using improved approximate approaches. Motonaga [24] examined non-integrability in perturbed Hamiltonian systems including periodically forced Duffing equations. These studies reveal the rich dynamics of nonlinear vibration systems and also illustrate the limitations of purely analytical or perturbation-based procedures when strong nonlinearity, forcing, delay, or long-time behavior is involved. Fractional and memory-dependent systems form another important class of differential equations. More recently, Yıldız et al. [25] considered fractional SDOF systems and applied the method of multiple time scales to obtain approximate analytical solutions for fractionally damped models. Burqan et al. [26] developed the ARA-residual power series method for time-fractional PDEs.

In addition, delay differential equations have also been widely studied due to their ability to model hereditary, feedback, and time-lag effects. Sezer et al. [27] developed a Taylor polynomial method for generalized pantograph equations with retarded or advanced arguments. Bahşı et al. [28] proposed an orthoexponential polynomial collocation method for high-order linear delay differential equations and included residual-based error analysis. Çevik et al. [29] developed an exponential collocation method for second-order linear delay differential equations, including delay terms in restoring force, damping, and acceleration. These studies are particularly relevant for the present work because they show that polynomial-based approaches can be successfully adapted to systems with delayed arguments, provided that the history-dependent term is treated carefully.

Taylor-series-based methods have long been recognized as systematic high-order tools for solving differential equations. Gülsu and Sezer [30] developed Taylor polynomial solutions for linear difference equations with variable coefficients, while Gülsu and Sezer [31] introduced Taylor polynomial approximations for differential-difference equations under mixed conditions. Kurt and Çevik [32] applied the Taylor matrix method to SDOF vibration systems, converting the governing equation into a system of algebraic equations for Taylor coefficients. Çevik [33] extended Taylor polynomial matrix techniques to longitudinal vibration of rods, and Bahşı and Çevik [34] applied a Taylor polynomial matrix method to RLC circuits. These early studies established the practicality of Taylor matrix formulations in mechanical and electrical vibration models. Later, Savaşaneril [35] proposed a Lucas polynomial matrix method for SDOF systems, and Yüzbaşı and Çetin [36] presented a Boubaker collocation method for SDOF systems, showing that polynomial matrix approaches remain relevant for vibration applications. Çevik et al. [37] reviewed polynomial matrix collocation methods in engineering and scientific applications, emphasizing their broad applicability to ODEs, PDEs, integral equations, fractional equations, and engineering models.

Recent studies have also advanced Taylor-type and residual-based formulations. Çayan et al. [38] proposed the Taylor-Splitting Collocation Method, where the fundamental Taylor matrix equation is reformulated through interval splitting and residual error estimation; this approach was applied to several mechanical vibration models. Aghazadeh et al. [39] used Taylor wavelet collocation to solve Emden–Fowler equations, while Al-Nana et al. [40] introduced an enhanced Taylor method for initial value problems by optimizing Taylor-series correction procedures. Pakdemirli [41] investigated two-point Taylor series expansions and discussed convergence behavior for truncated Taylor representations. Boscarino and Macca [42] developed adaptive Taylor-based schemes for stiff ODEs, highlighting the relevance of adaptive Taylor formulations for stability and accuracy. Taylor et al. [43] proposed an adaptive Deep Fourier Residual method using overlapping domain decomposition, and Liu and Liu [44] developed a forward progressive PINN with Taylor series expansion, where Taylor formulas and time-domain decomposition were incorporated into physics-informed learning. These studies are particularly close to the present work because they combine, in different ways, Taylor expansion, residual evaluation, adaptivity, and domain decomposition concepts.

The literature therefore shows several important but separate developments. Taylor and polynomial matrix methods provide high-order local approximations and algebraic formulations [30–34,37]. Residual-based approaches improve error monitoring and solution reliability in fractional and collocation contexts [26,28]. Adaptive and domain-decomposition ideas enhance long-time solution stability and computational efficiency [38,42–44]. PINN-based studies demonstrate the usefulness of physics residuals as accuracy indicators and training objectives [1–3]. Nonlinear vibration studies reveal the need for methods that remain stable for strong nonlinearity, fractional damping, delay, and parametric excitation [5,6,15,17–22,24,25,45–47].

Despite these advances, a clear research gap remains. Existing Taylor-based methods generally use fixed expansion intervals or predetermined splitting strategies, and they may lose accuracy when the solution interval becomes long or when nonlinear effects intensify. Residual-based methods are often developed as separate analytical or semi-analytical schemes rather than as adaptive continuation mechanisms for Taylor approximations. PINN-inspired residual monitoring has not been systematically integrated into a classical Taylor polynomial marching framework. Moreover, overlapping interval continuation, adaptive step-size control, residual acceptance criteria, and high-order Taylor recurrence are rarely unified into a single method applicable to nonlinear, fractional, and parametrically excited SDOF systems.

To address this gap, the present study proposes the Adaptive Residual-Controlled Overlapping Taylor (ARCOT) method. ARCOT constructs a high-order Taylor polynomial locally on each subinterval but accepts only a reliable interior portion of that expansion. The next expansion begins from this interior continuation point, producing an overlapping time-marching structure. A physics-based residual, inspired by residual minimization concepts used in PINNs, is evaluated on each segment. If the residual exceeds a prescribed tolerance, the segment is rejected, and the step size is reduced; if the residual is sufficiently small, the segment is accepted, and the step size may be increased. In this way, ARCOT combines high-order Taylor approximation, residual-based stabilization, adaptive interval selection, and overlapping continuation within one framework.

The originality of the present study lies in the systematic integration of these elements and in the comparative application of ARCOT to several nonlinear vibration models, including Duffing, Van der Pol, cubic–quintic, and Mathieu-type differential equations. Unlike conventional Taylor matrix methods, ARCOT is not limited to a single global expansion or a fixed splitting pattern. Unlike standard Runge–Kutta methods, it employs high-order local polynomial information. Unlike PINNs, it does not require training neural networks but still uses a physics-residual criterion to monitor solution quality. Thus, ARCOT provides a bridge between classical Taylor-series numerical methods, adaptive residual-based algorithms, and modern physics-informed computational ideas.

More specifically, ARCOT differs from conventional adaptive Taylor methods by combining high-order local Taylor reconstruction with residual-controlled interval adaptation and interior-point overlapping continuation. In contrast to adaptive Runge–Kutta methods, which regulate the integration step through embedded local truncation-error estimates, ARCOT directly uses the governing-equation residual as the acceptance–rejection and interval-regulation criterion. Moreover, unlike residual-based approaches in which the residual primarily serves as an error indicator or correction measure, ARCOT integrates residual evaluation directly into the continuation mechanism. Thus, the methodological distinction of ARCOT lies in the unified interaction of Taylor reconstruction, residual-controlled adaptivity, and overlapping continuation.

2. Mathematical Formulation of Nonlinear Oscillators

2.1. General Nonlinear Polynomial Oscillator

A broad class of nonlinear vibration systems encountered in mechanics and engineering may be represented by the following generalized nonlinear SDOF equation:

$$m\ddot{x}(t) + c\dot{x}(t) + g(x) = F(t) \tag{1}$$

where $x(t)$ denotes the displacement response of the system, m is the mass coefficient, c represents the damping coefficient, $g(x)$ denotes the restoring force term containing linear and nonlinear stiffness components, and $F(t)$ is the external excitation function. The dots indicate differentiation with respect to time t.

In many nonlinear vibration problems, the restoring force can be approximated by a polynomial function of the displacement. Accordingly, the nonlinear restoring term considered in the present study is expressed as

$$g(x) = kx + \alpha x^3 + \beta x^5 \tag{2}$$

where k is the linear stiffness coefficient, α is the cubic nonlinear stiffness parameter, and β is the quintic nonlinear stiffness parameter. Substituting Equation (2) into Equation (1) yields the generalized nonlinear polynomial oscillator equation:

$$m\ddot{x}(t) + c\dot{x}(t) + kx(t) + \alpha x^3(t) + \beta x^5(t) = F(t) \tag{3}$$

This formulation provides a unified representation for several important nonlinear oscillators widely studied in vibration theory and nonlinear dynamics.

When the quintic nonlinear coefficient is neglected, i.e., $\beta = 0$; Equation (3) reduces to the classical Duffing oscillator:

$$m\ddot{x}(t) + c\dot{x}(t) + kx(t) + \alpha x^3 = F_0 cos(\omega t) \tag{4}$$

where F_0 and ω denote the forcing amplitude and excitation frequency, respectively. The Duffing equation is one of the most extensively studied nonlinear vibration models because of its ability to exhibit hardening, softening, bifurcation, jump phenomena, and chaotic responses depending on the system parameters.

If the quintic nonlinear term is retained, Equation (3) is called the cubic–quintic oscillator equation. The inclusion of the quintic term allows the model to represent stronger nonlinear restoring characteristics and more complex dynamic behavior. Cubic–quintic oscillators arise in nonlinear structural systems, nonlinear optics, microelectromechanical systems, plasma physics, and strongly nonlinear vibration models.

The generalized polynomial representation given in Equation (3) is particularly suitable for the proposed ARCOT method because polynomial nonlinearities can be incorporated directly into Taylor-series recurrence relations through systematic coefficient operations. Consequently, both Duffing and cubic–quintic oscillators may be treated within a unified computational framework without altering the fundamental ARCOT formulation.

2.2. Van der Pol Oscillator

The Van der Pol oscillator is one of the most fundamental nonlinear dynamical systems used to model self-excited oscillations and nonlinear damping phenomena. Originally introduced in the study of electrical circuits containing vacuum tubes, the Van der Pol equation has subsequently found applications in mechanics, biology, acoustics, control systems, fluid dynamics, and nonlinear vibration theory. Unlike classical linear oscillators, the Van der Pol system contains a displacement-dependent damping mechanism that injects energy into the system at small amplitudes while dissipating energy at larger amplitudes, thereby generating stable self-sustained oscillations known as limit cycles.

The dimensionless form of the Van der Pol oscillator considered in the present study is given by

$$\ddot{x}(t) - \mu\big(1 - x^2(t)\big)\dot{x}(t) + x(t) = 0 \tag{5}$$

where $x(t)$ denotes the displacement response and μ is the nonlinear damping parameter controlling the strength of the nonlinearity. The overdots represent differentiation with respect to time t.

The nonlinear damping term $-\mu(1 - x^2)\dot{x}$ constitutes the characteristic feature of the Van der Pol equation. For small displacement amplitudes satisfying $|x| < 1$, the quantity $(1 - x^2)$ remains positive, resulting in negative effective damping and energy input into the system. Conversely, when $|x| > 1$, the damping becomes positive, and energy is dissipated. This nonlinear energy exchange mechanism causes the solution trajectories to converge toward a stable periodic orbit regardless of the initial conditions.

The dynamic behavior of the Van der Pol oscillator strongly depends on the parameter μ. For small μ, the system behaves similarly to a weakly nonlinear harmonic oscillator, whereas larger μ values produce strongly nonlinear relaxation oscillations characterized by slow motions and rapid transitions. Such behavior poses significant challenges for numerical methods, as conventional fixed-step schemes may suffer from reduced efficiency or stability over long integration intervals.

The Van der Pol oscillator is particularly suitable for evaluating the performance of the proposed ARCOT method because the nonlinear damping mechanism generates continuously evolving local dynamics throughout the solution interval. Consequently, the equation provides an effective benchmark for assessing the adaptive interval selection, residual-control mechanism, and overlapping continuation strategy employed in the ARCOT framework.

2.3. Mathieu Equation

The Mathieu equation is a classical model for parametrically excited dynamical systems and appears in applications such as vibrating structures, rotating shafts, MEMS devices, pendulum systems, and electrical circuits with periodically varying parameters. In contrast to externally forced oscillators, the Mathieu equation contains a time-dependent stiffness term that may induce parametric resonance and instability.

The generalized damped Mathieu equation considered in this study is given by

$$m\ddot{x}(t) + c\dot{x}(t) + \left(k + q cos(\Omega_m t)\right)x(t) = F_0 cos(\omega t) \tag{6}$$

where m is the mass coefficient, c is the damping coefficient, k denotes the mean stiffness, q is the parametric excitation amplitude, and Ω_m is the parametric excitation frequency. The right-hand-side term represents an external harmonic excitation with amplitude F_0 and frequency ω.

The periodically varying stiffness term $\left(k + q cos(\Omega_m t)\right)$ may generate stable, unstable, or amplified oscillatory responses depending on the system parameters. In the absence of damping and external forcing, Equation (6) reduces to the classical Mathieu equation,

$$\ddot{x}(t) + \left(\delta + \epsilon cos(\Omega_m t)\right)x(t) = 0 \tag{7}$$

which is well known for its characteristic stability and instability regions.

Because Mathieu-type systems are highly sensitive near parametric resonance boundaries, they provide an effective benchmark for evaluating the adaptive continuation and residual-control capabilities of the proposed ARCOT method.

3. Adaptive Residual-Controlled Overlapping Taylor (ARCOT) Method

3.1. Classical Taylor Expansion

In the proposed ARCOT framework, the solution is approximated locally by a truncated Taylor series expansion about the point t_i:

$$x(t) = \sum_{n=0}^{N} a_n (t - t_i)^n \tag{8}$$

where N denotes the truncation order and a_n are the Taylor coefficients. The corresponding first and second derivatives are given by

$$\dot{x}(t) = \sum_{n=1}^{N} n a_n (t - t_i)^{n-1} \tag{9a}$$

and

$$\ddot{x}(t) = \sum_{n=2}^{N} n(n-1) a_n (t - t_i)^{n-2} \tag{9b}$$

respectively. Substituting these expressions into the governing differential equation yields recurrence relations for the unknown Taylor coefficients.

3.2. Taylor Recurrence Relations

The Taylor coefficients are obtained by substituting the truncated Taylor expansion into the governing differential equation and equating coefficients of identical powers of $(t - t_i)$. Let the initial coefficients be

$$a_0 = x(t_i), \;\; a_1 = \dot{x}(t_i), \tag{10}$$

The remaining coefficients are determined recursively according to the oscillator model under consideration.

3.2.1. Duffing Oscillator

For the Duffing Equation (4), the recurrence relation becomes

$$a_{n+2} = \frac{f_n - c(n+1)a_{n+1} - ka_n - \alpha(x^3)_n}{m(n+2)(n+1)} \tag{11}$$

where f_n denotes the Taylor coefficient of the forcing function and $(x^3)_n$ represents the n-th coefficient of the cubic polynomial expansion.

3.2.2. Cubic–Quintic Oscillator

For the cubic–quintic oscillator (3), the recurrence relation is written as

$$a_{n+2} = \frac{f_n - c(n+1)a_{n+1} - ka_n - \alpha(x^3)_n - \beta(x^5)_n}{m(n+2)(n+1)} \tag{12}$$

where $(x^5)_n$ denotes the quintic polynomial coefficient.

3.2.3. Van der Pol Oscillator

For the Van der Pol Equation (5), the recurrence relation becomes

$$a_{n+2} = \frac{\mu[(\dot{x})_n - (x^2\dot{x})_n] - a_n}{(n+2)(n+1)} \tag{13}$$

where $(x^2\dot{x})_n$ denotes the coefficient associated with the nonlinear damping term.

3.2.4. Mathieu Equation

For the Mathieu Equation (6), the recurrence relation is obtained as

$$a_{n+2} = \frac{f_n - c(n+1)a_{n+1} - ka_n - q(\cos(\Omega_m t)\, x)_n}{m(n+2)(n+1)} \tag{14}$$

where $(\cos(\Omega_m t)\, x)_n$ denotes the coefficient generated by the parametric excitation term.

The recurrence relations above form the basis of the local Taylor expansions employed in the proposed ARCOT framework.

3.3. Overlapping Continuation Strategy

In conventional Taylor-series marching methods, the solution obtained at the endpoint of a local expansion interval is directly used as the initial condition for the subsequent interval. However, truncation errors tend to accumulate near the interval boundary, particularly for strongly nonlinear systems and long integration intervals. To reduce this effect, the proposed ARCOT method employs an overlapping continuation strategy.

Let the Taylor expansion be constructed over the interval.

$$[t_i, t_i + H] \tag{15}$$

where H denotes the local expansion length. Instead of advancing the solution from the endpoint $t_i + H$, only an interior portion of the interval is accepted, and the next expansion is initiated from the continuation point

$$t_{i+1} = t_i + \theta H, \;\; 0 < \theta < 1 \tag{16}$$

where θ is the overlap parameter. Consequently, consecutive Taylor expansions partially overlap as seen in Figure 1.

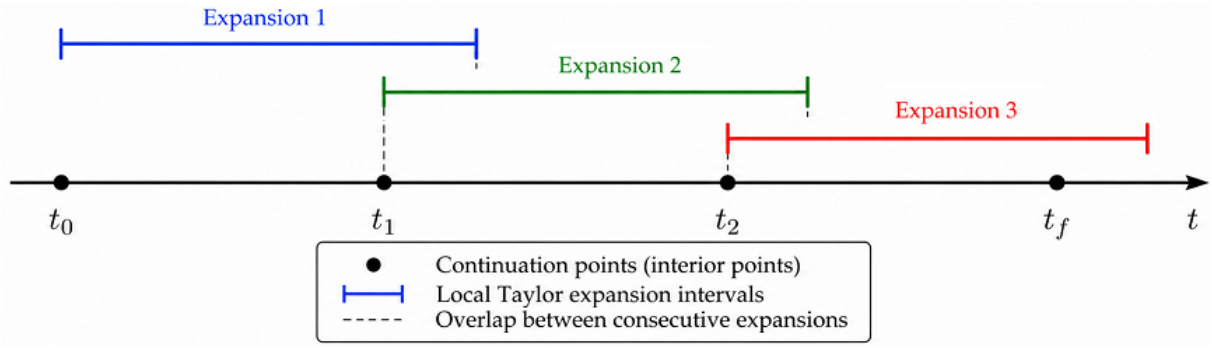

Figure 1. Schematic representation of the overlapping continuation strategy employed in the ARCOT method.

In the present implementation, the continuation point is selected from an interior collocation/grid point of the current Taylor interval. This strategy reduces the influence of boundary truncation errors, improves local stability, and suppresses cumulative error propagation during long-time integration.

The overlapping continuation mechanism constitutes one of the principal features distinguishing the ARCOT method from conventional Taylor marching procedures.

3.4. Residual-Controlled Adaptivity

To monitor the accuracy and stability of the local Taylor approximations, the ARCOT method employs a residual-based adaptive control strategy. After constructing the local Taylor expansion over a given interval, the approximate solution is substituted back into the governing differential equation to compute the residual function.

For a general nonlinear oscillator, the residual may be written as

$$R(t) = m\ddot{x}(t) + c\dot{x}(t) + g(x(t)) - F(t) \tag{17}$$

where $x(t)$ denotes the local Taylor approximation. Accordingly, the residual functions for the oscillator models considered in this study are defined as follows.

For the Duffing oscillator,

$$R(t) = m\ddot{x}(t) + c\dot{x}(t) + kx(t) + \alpha x^3 - F(t) \tag{18}$$

for the cubic–quintic oscillator,

$$R(t) = m\ddot{x}(t) + c\dot{x}(t) + kx(t) + \alpha x^3 + \beta x^5 - F(t) \tag{19}$$

for the Van der Pol oscillator,

$$R(t) = \ddot{x}(t) - \mu\big(1 - x^2(t)\big)\dot{x}(t) + x(t) \tag{20}$$

and for the Mathieu equation,

$$R(t) = m\ddot{x}(t) + c\dot{x}(t) + \big(k + qcos(\Omega_m t)\big)x(t) - F(t) \tag{21}$$

The local Taylor segment is accepted if the residual satisfies.

$$\max_{t\in[t_i, t_i+\theta H]} |R(t)| < \varepsilon \tag{22}$$

where ε denotes a prescribed residual tolerance. Otherwise, the interval is rejected and recomputed using a smaller step size. In this manner, the residual function serves as a physics-based accuracy indicator controlling the adaptive continuation process of the ARCOT method.

3.5. Adaptive Step-Size Strategy

The ARCOT method employs an adaptive step-size strategy to improve numerical stability and maintain the residual error within a prescribed tolerance throughout the solution interval. After constructing a local Taylor expansion and evaluating its residual, the corresponding segment is either accepted or rejected according to the residual criterion defined in the previous section.

If the residual satisfies

$$\max|R(t)| < \varepsilon \tag{23}$$

the segment is accepted, and the continuation process proceeds to the next overlapping interval. In regions where the residual remains significantly smaller than the prescribed tolerance, the local expansion interval may be enlarged to improve computational efficiency.

Conversely, if the residual exceeds the tolerance limit,

$$\max|R(t)| \geq \varepsilon \tag{24}$$

the segment is rejected, and the interval length is reduced before recomputing the Taylor expansion. This adaptive reduction mechanism prevents excessive truncation errors and suppresses instability growth in strongly nonlinear or rapidly varying regions.

The adaptive interval length is bounded by $H_{\min} \leq H \leq H_{\max}$, where $H_{\min}$ and $H_{\max}$ denote the prescribed minimum and maximum expansion lengths, respectively, and the continuation process starts with an initial expansion length H_0. Within these bounds, H is dynamically adjusted during the continuation process according to the residual criterion. Stable solution regions generally permit larger intervals, whereas strongly nonlinear or sensitive regions require smaller intervals to maintain solution accuracy. In this way, the adaptive step-size strategy provides local stability control while simultaneously improving long-time integration performance and the computational robustness of the ARCOT framework.

3.6. ARCOT Algorithm

The overall computational procedure of the ARCOT method is summarized in Algorithm 1. The method starts from the prescribed initial conditions and advances the solution by constructing local Taylor expansions over overlapping intervals. At each step, the residual is evaluated to determine whether the current segment should be accepted or recomputed with a smaller interval.

Algorithm 1. ARCOT Method

1. Initialize $t_0, x(t_0), \dot{x}(t_0), H, N$, and ε.
2. Construct the local Taylor expansion over $[t_i, t_i + H]$.
3. Compute Taylor coefficients recursively.
4. Evaluate the residual function $R(t)$.
5. If $\max|R(t)| < \varepsilon$ then:
    - accept the segment,
    - select the interior continuation point,
    - update the solution state,
    - optionally enlarge the interval.
6. Otherwise:
    - reject the segment,
    - reduce the interval length,
    - recompute the Taylor expansion.
7. Repeat until $t_i \geq t_f$.

In this algorithm, the parameter θ determines the interior continuation point and therefore controls the amount of overlap between consecutive Taylor expansions. The residual tolerance ε governs the acceptance or rejection of each local segment. Thus, the algorithm combines high-order Taylor approximation, residual-based error control, and overlapping continuation within a single adaptive framework.

3.7. Computational Aspects

The computational cost of the ARCOT method depends mainly on the Taylor expansion order, the number of adaptive segments, and the residual evaluation procedure. For a Taylor polynomial of order N, the coefficient recursion requires $O(N)$ operations for linear terms, while nonlinear polynomial terms introduce additional convolution-type computations. Since the method advances locally over adaptive intervals, the overall cost remains moderate for the nonlinear oscillators considered herein.

The convergence behavior is governed by the Taylor order and local interval length. Higher-order expansions generally improve local accuracy, whereas excessively large intervals may amplify truncation errors near interval boundaries. The proposed overlapping continuation strategy mitigates this effect by advancing the solution from an interior continuation point rather than the interval endpoint.

Numerical stability is primarily controlled through the residual-based adaptive mechanism. In regions with strong nonlinearities or rapidly varying responses, the residual increases and the interval length is automatically reduced. Conversely, smoother regions permit larger intervals, thereby improving computational efficiency while maintaining accuracy.

Unlike classical Taylor marching methods, which connect consecutive expansions directly at interval endpoints, ARCOT employs overlapping continuation between adjacent segments. The overlap ratio, controlled by the parameter θ, influences both stability and efficiency. Smaller θ values increase overlap and generally improve stability, whereas larger values reduce computational cost but may increase sensitivity to truncation errors.

Although residual evaluation introduces additional computations, it provides a direct physics-based measure of local approximation quality and enables effective adaptive control without requiring excessively small global step sizes.

4. Numerical Applications

In this section, the performance of the proposed ARCOT method is investigated through several nonlinear oscillator models, including Duffing, cubic–quintic, Van der Pol, and Mathieu equations. The numerical examples are selected to assess the accuracy, stability, and adaptive capabilities of the method under different nonlinear dynamic behaviors.

For each problem, the governing equation is solved over a prescribed time interval using the ARCOT framework. The obtained results are presented in terms of displacement responses, phase-plane trajectories, residual histories, and adaptive interval evolution. In addition, comparisons with classical Runge–Kutta-based solutions are provided to evaluate the accuracy and robustness of the proposed method.

Unless otherwise stated, the residual tolerance, Taylor expansion order, and overlap parameters are selected consistently throughout the numerical studies to provide a unified evaluation framework for the ARCOT methodology.

4.1. Duffing Oscillator

In this example, the accuracy and effectiveness of the proposed ARCOT method are investigated for a harmonically excited undamped Duffing oscillator. The problem represents a nonlinear vibration system with cubic stiffness nonlinearity and periodic external excitation, providing a classical benchmark for nonlinear numerical methods.

Example 1. *The governing equation is given by*

$$\ddot{x}(t) + \frac{k}{m}(x) + \frac{k^*}{2mh^2}x^3 = \frac{F_0}{m}\sin\omega_0 t$$

subject to the initial conditions

$$x(0) = A,\ \ \dot{x}(0) = 0$$

where

$$k = 300\frac{N}{m}, k^* = \frac{200N}{m}, m = 10\text{ kg}, h = 0.8\text{ m}, F_0 = 1\text{ N}, \omega_0 = \frac{2\text{rad}}{\text{s}}, A = 0.5\text{ m}$$

For the ARCOT computation, a Taylor expansion of order $N = 30$ was employed with a residual tolerance of $\varepsilon = 10^{-2}$. Each full Taylor interval was discretized using 30 uniformly spaced continuation points, and the next expansion was initiated from point 15, corresponding to $\theta = 15/29 \approx 0.5172$. The residual was evaluated at 100 uniformly spaced points over the accepted portion of each interval. The initial full interval length was $H_0 = 0.25$, with $H_{\min} = 10^{-6}$ and $H_{\max} = 0.50$. The RK4 reference solution was computed using a fixed step size of 5×10^{-4}.

ARCOT completed the solution with 66 accepted intervals and no rejected intervals, with maximum and mean residuals of 4.5898×10^{-4} and 3.1644×10^{-5}, respectively. The computational times were approximately 2.67 s for ARCOT and 0.49 s for RK4.

The equation is solved using the proposed ARCOT framework, and the obtained numerical results are compared with the variational approach of Bayat and Pakar [7], the Taylor-Splitting method of Çayan et al. [38], the classical Runge–Kutta solution, and the Energy Balance Method (EBM) reported by Mehdipour et al. [16]. The comparison results are presented in Table 1.

As observed in Table 1, the ARCOT results exhibit excellent agreement with the reference Runge–Kutta solutions throughout the considered interval. In most cases, the obtained values also remain highly consistent with the Taylor-Splitting and variational solutions reported in the literature. Minor deviations observed in some EBM results become more noticeable at larger time values due to the strongly nonlinear oscillatory behavior of the system.

The obtained results demonstrate that the overlapping continuation and residual-controlled adaptive strategy employed in ARCOT successfully maintains numerical stability and high accuracy over long integration intervals. The method accurately captures the nonlinear oscillatory dynamics generated by the cubic stiffness term without exhibiting noticeable error accumulation.

Table 1. Comparison of ARCOT results with Runge–Kutta, Taylor–Splitting, variational, and EBM solutions available in the literature.

t	ARCOT	Runge-Kutta	Taylor-Splitting [38]	Variational [7]	EBM [16]
0.00	0.50000000	0.50000000	0.5000	0.5	0.5
0.40	−0.32690399	−0.32690848	−0.3270	−0.3290	−0.3292
0.80	−0.05634365	−0.05634518	−0.0559	−0.0695	−0.0688
1.20	0.41187140	0.41188189	0.4115	0.4169	0.4165
1.60	−0.48513684	−0.48514688	−0.4853	−0.4855	−0.4855
2.00	0.22644847	0.22645092	0.2273	0.2462	0.2450
2.40	0.17335542	0.17335548	0.1722	0.1535	0.1555
2.80	−0.46940250	−0.46940832	-	−0.4608	−0.4614
3.20	0.44072530	0.44073446	-	0.4400	0.4402
3.60	−0.11318792	−0.11319070	-	−0.0868	−0.0893
4.00	−0.28056043	−0.28056796	-	−0.3206	−0.3179
4.40	0.49861371	0.49862748	-	0.4991	0.4990
4.80	−0.36995569	−0.36995741	-	−0.3788	−0.3783

As shown in Figure 2a–c, the ARCOT displacement response closely agrees with the RK4 reference solution throughout the integration interval, while the corresponding phase-plane trajectories are nearly coincident. The small absolute error relative to RK4 further confirms the accuracy of the ARCOT solution for the harmonically excited Duffing oscillator.

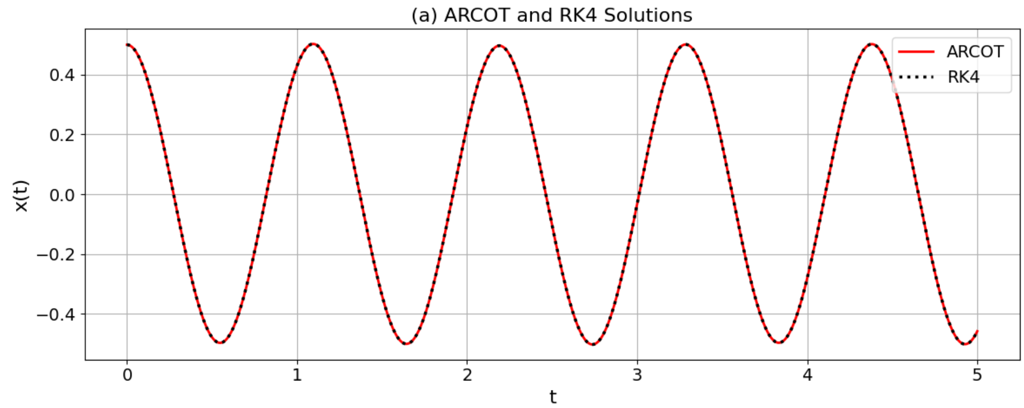

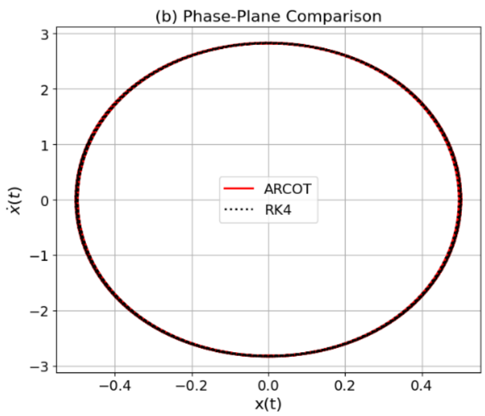

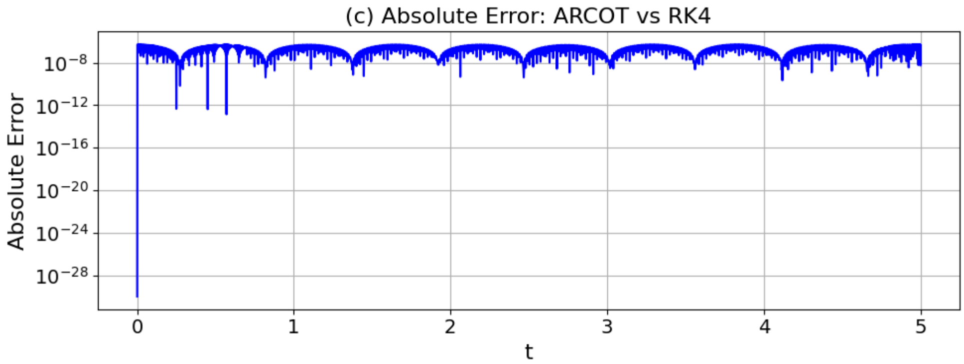

Figure 2. Numerical performance of ARCOT for the harmonically excited Duffing oscillator: (**a**) displacement responses obtained by ARCOT and RK4; (**b**) corresponding phase-plane trajectories; and (**c**) absolute error of the ARCOT solution relative to the RK4 reference solution over the integration interval.

4.2. Cubic–Quintic Oscillator

In this example, the performance of the proposed ARCOT method is investigated for a strongly nonlinear cubic–quintic Duffing equation. The inclusion of the quintic stiffness term produces stronger nonlinear restoring characteristics compared with the classical Duffing oscillator and therefore provides a more demanding benchmark for assessing the robustness and stability of the numerical method.

Example 2. *The cubic–quintic oscillator considered in this study is given by*

$$\ddot{x}(t) + x + 5x^3 + x^5 = 0$$

subject to the initial conditions

$$x(0) = 1,\ \dot{x}(0) = 1$$

For this example, the ARCOT computation employed $N = 30$, $\varepsilon = 10^{-2}$, and $\theta = 15/29 \approx 0.5172$. The full Taylor interval contained 30 uniformly spaced continuation points, while the residual was evaluated at 100 uniformly spaced points over the accepted interval. The initial interval length was $H_0 = 0.15$, with $H_{\mathrm{min}} = 10^{-6}$ and $H_{\mathrm{max}} = 0.30$. The RK4 reference solution was computed using a fixed step size of 5×10^{-4}.

The equation is solved using the proposed ARCOT framework and subsequently compared with the Jacobi elliptic function solution reported by Salas et al. [46] together with the classical RK4 solution.

ARCOT completed the solution with 78 accepted intervals and no rejected intervals, with maximum and mean residuals of 1.286×10^{-13} and 9.042×10^{-15}, respectively. The computational times were approximately 3.29 s for ARCOT and 0.89 s for RK4.

As shown in Figure 3a–c, the ARCOT displacement response closely agrees with both the RK4 and Jacobi elliptic solutions throughout the integration interval, while the nearly coincident phase-plane trajectories in Figure 3b demonstrate that ARCOT accurately preserves the nonlinear oscillatory dynamics. Figure 3c further shows that the absolute errors of ARCOT and RK4 relative to the Jacobi elliptic solution remain small and exhibit nearly identical behavior. These results confirm the accuracy and robustness of ARCOT in the presence of strong polynomial nonlinearities. The quintic nonlinear term increases the strength of the nonlinearity and may amplify truncation errors in conventional Taylor marching procedures, particularly near interval boundaries. In ARCOT, the overlapping continuation and residual-controlled adaptive strategy limits cumulative error propagation by adjusting the local continuation interval according to the residual behavior, thereby maintaining stable and accurate integration.

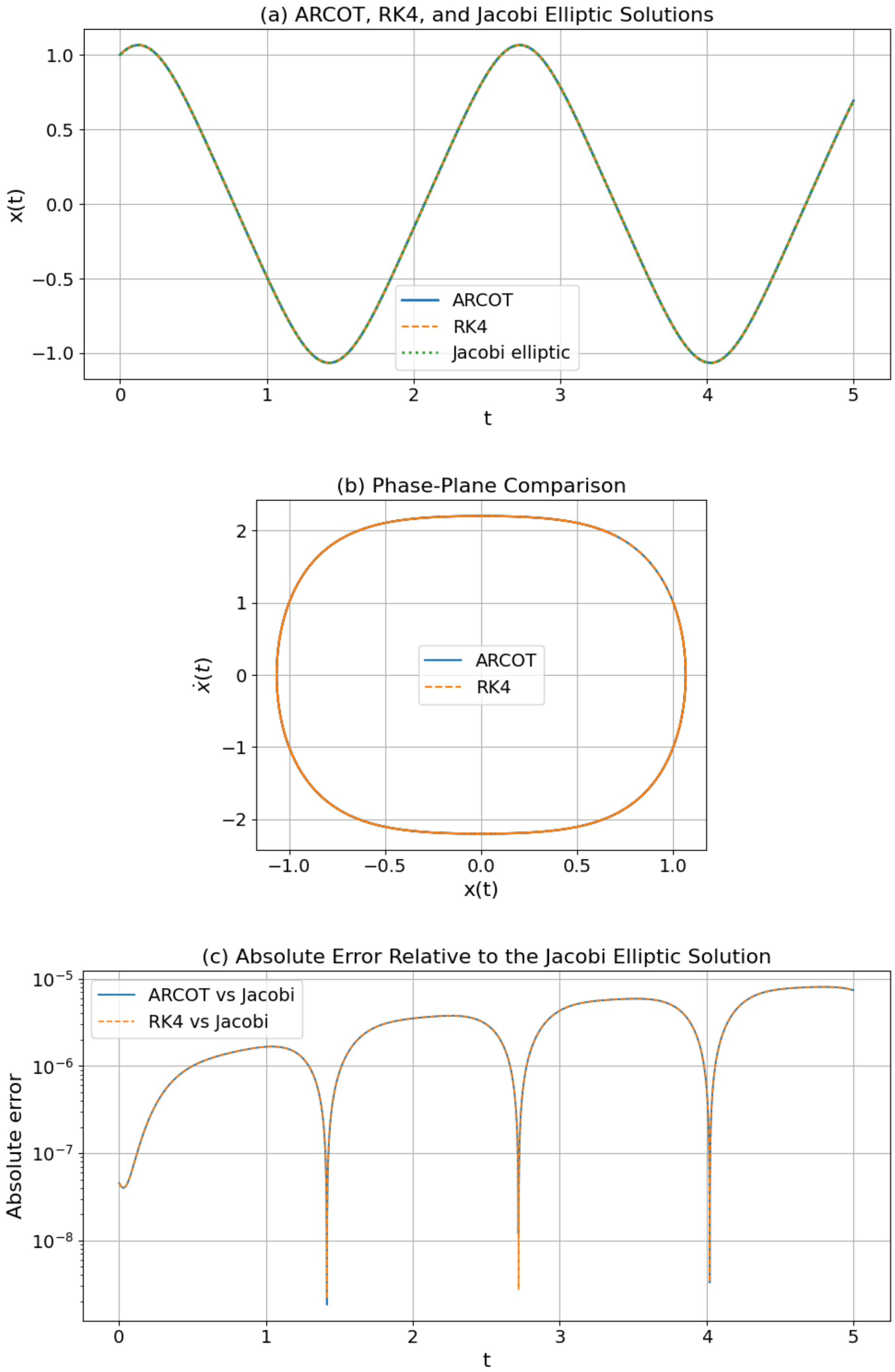

Figure 3. Numerical performance of ARCOT for the cubic–quintic oscillator: (**a**) displacement responses obtained by ARCOT, RK4, and the Jacobi elliptic solution; (**b**) phase-plane comparison of ARCOT and RK4; and (**c**) absolute errors of the ARCOT and RK4 solutions relative to the Jacobi elliptic solution.

4.3. Van der Pol Oscillator

In this example, the performance of the proposed ARCOT method is examined for a forced Van der Pol–Duffing–quintic oscillator containing nonlinear damping, cubic stiffness nonlinearity, quintic restoring effects, and external harmonic excitation. The simultaneous presence of nonlinear damping and higher-order polynomial stiffness terms produces a strongly nonlinear dynamic system with amplitude-dependent behavior and continuously evolving local dynamics.

Example 3. *The governing equation is given by*

$$\ddot{x}(t) - \mu(1 - x^2)\dot{x} + \omega_0^2 x + \alpha x^3 + \lambda x^5 = F\cos(\omega t)$$

subject to the initial conditions

$$x(0) = 0.5, \ \ \dot{x}(0) = 0$$

Following the work in [22], the system parameters are chosen as follows

$$\mu = -0.5, \omega_0 = 4, \alpha = 1.5, \lambda = 0.1, F = 0.02, \omega = 1.5$$

The nonlinear damping term $\mu(1 - x^2)$ introduces amplitude-dependent energy dissipation and excitation characteristics, leading to non-uniform oscillatory behavior and limit-cycle-type evolution. In addition, the cubic and quintic stiffness terms further strengthen the nonlinear response and increase the sensitivity of the solution to local truncation errors.

The ARCOT computation was performed using a Taylor order of $N = 30$, a residual tolerance of $\varepsilon = 10^{-2}$, and an overlap parameter of $\theta = 15/29 \approx 0.5172$. 30 uniformly spaced points were used for continuation-point selection, and the residual was evaluated at 100 uniformly spaced points over each accepted interval. The initial interval length was $H_0 = 0.10$, with $H_{\min} = 10^{-6}$ and $H_{\max} = 0.25$. The RK4 reference solution employed a fixed step size of 5×10^{-4}.

ARCOT completed the solution with 277 accepted intervals and no rejected intervals, with maximum and mean residuals of 5.784×10^{-15} and 5.229×10^{-16}, respectively. The computational times were approximately 9.96 s for ARCOT and 1.95 s for RK4.

As shown in Figure 4a–c, the transient displacement responses obtained by ARCOT and RK4 exhibit excellent agreement throughout the integration interval, demonstrating the accuracy of ARCOT for an oscillator with combined nonlinear damping and higher-order stiffness nonlinearities. The nearly coincident phase-plane trajectories in Figure 4b further show that ARCOT preserves the nonlinear dynamic behavior of the system, while the small absolute error relative to the RK4 reference solution in Figure 4c confirms the close numerical agreement between the two methods. The residual-controlled adaptive continuation mechanism further supports stable integration by adjusting the local interval length according to the evolving nonlinear response.

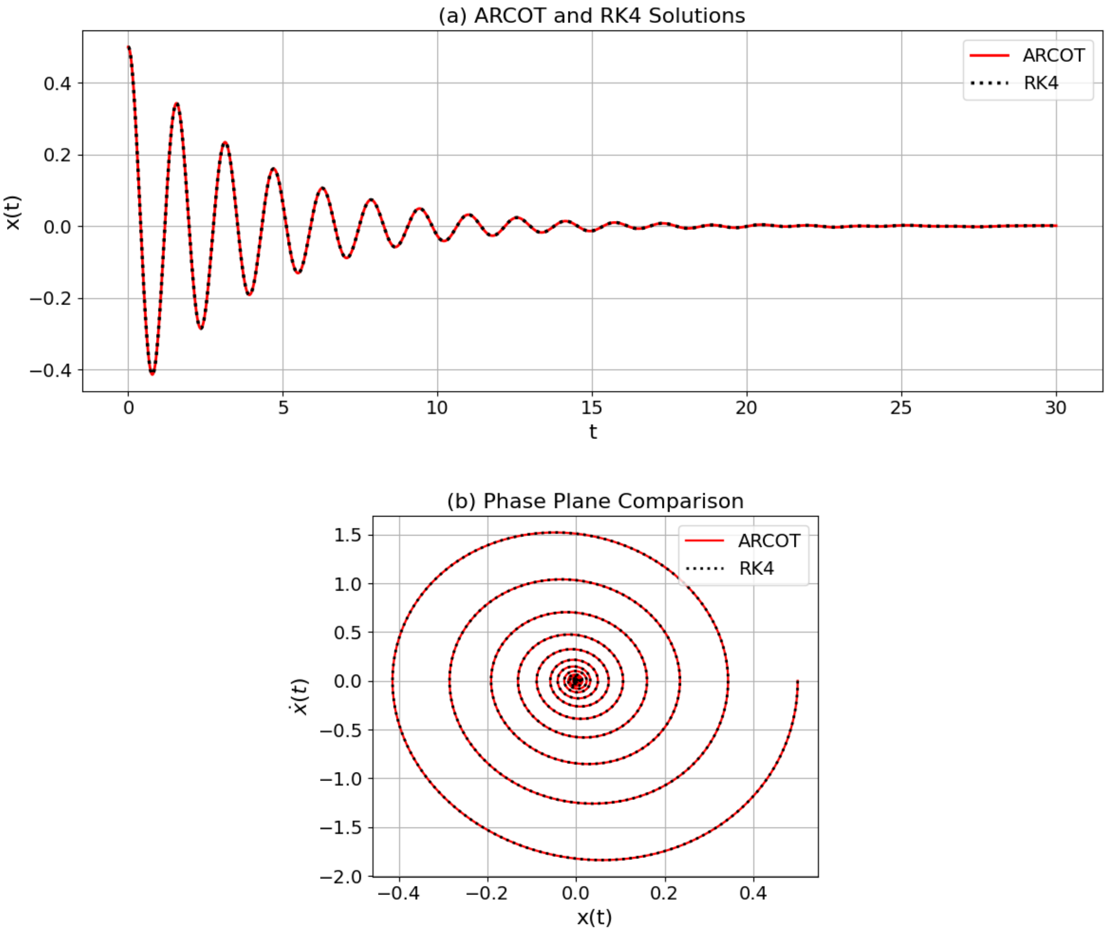

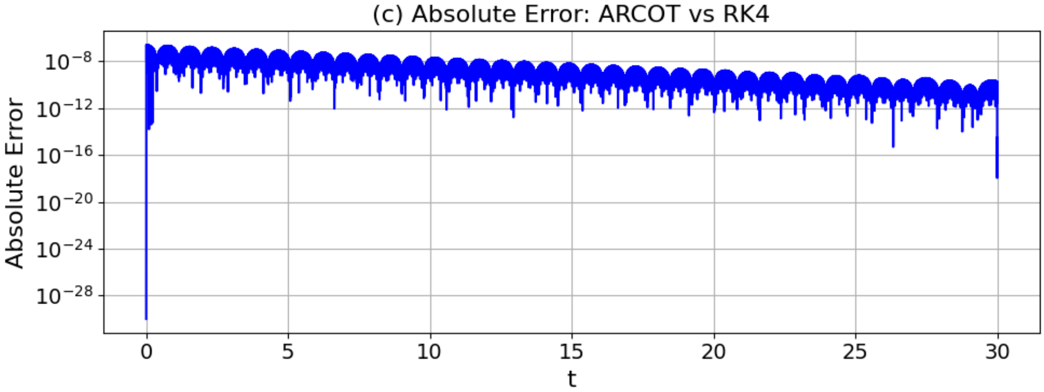

Figure 4. Numerical performance of ARCOT for the forced Van der Pol–Duffing–quintic oscillator: (**a**) displacement responses obtained by ARCOT and RK4; (**b**) corresponding phase-plane trajectories; and (**c**) absolute error of the ARCOT solution relative to the RK4 reference solution.

4.4. Mathieu Equation

In this example, the performance of the proposed ARCOT method is investigated for an undamped nonlinear Mathieu-type pendulum equation exhibiting parametric excitation and stability-transition behavior.

Example 4. *As a representative parametrically excited nonlinear oscillator, the nonlinear Mathieu-type pendulum discussed in Ref. [48] is considered. The governing equation is given by*

$$\ddot{x}(t) + \left(\frac{g}{L} - \frac{A}{L}\cos t\right)\sin x = 0$$

where x denotes the angular displacement, g is the gravitational acceleration, L is the pendulum length, and $A\cos t$ represents the vertical motion of the support. For convenience, the equation is rewritten in the standard Mathieu-type form.

$$\ddot{x}(t) + (\delta + \epsilon\cos t)\sin x = 0$$

subject to the initial conditions

$$x(0) = 0.1,\ \ \dot{x}(0) = 0$$

The ARCOT solution was obtained using $N = 30$, $\varepsilon = 10^{-2}$, and $\theta = 15/29 \approx 0.5172$. 30 uniformly spaced continuation points were used within each full Taylor interval, and the residual was evaluated at 100 uniformly spaced points over the accepted portion. The initial interval length was $H_0 = 0.25$, with $H_{\min} = 10^{-6}$ and $H_{\max} = 0.50$.

Following [48], the parametric excitation amplitude is selected as $\epsilon = 0.05$, and two values of δ are considered to examine the unstable and stable dynamic regimes. For $\delta = 0.25$, the response exhibits amplitude growth associated with parametric instability, with the ARCOT and RK4 solutions showing close agreement throughout the integration interval (Figure 5a). In contrast, for $\delta = 0.30$, the response remains stable and bounded approximately within $-0.20 < x(t) < 0.20$, again with close agreement between the two methods (Figure 5b). The corresponding phase-plane trajectories for the unstable case are nearly coincident (Figure 5c), while the small absolute error of ARCOT relative to the RK4 reference solution further confirms their numerical agreement (Figure 5d). These results demonstrate that ARCOT successfully captures both the amplitude growth in the unstable regime and the bounded oscillatory response in the stable regime.

For the stable case, ARCOT completed the solution with 545 accepted intervals and no rejected intervals, with maximum and mean residuals of 4.857×10^{-17} and 1.832×10^{-17}, respectively. The computational times were approximately 84.21 s for ARCOT and 5.74 s for RK4. The maximum and mean absolute errors of ARCOT relative to the RK4 reference solution were 1.369×10^{-9} and 5.288×10^{-10}, respectively.

For the stable case, ARCOT completed the solution with 545 accepted intervals and no rejected intervals, with maximum and mean residuals of 2.776×10^{-16} and 4.858×10^{-17}, respectively. The computational times were approximately 183.62 s for ARCOT and 4.87 s for RK4. The maximum and mean absolute errors of ARCOT relative to the RK4 reference solution were 8.814×10^{-9} and 1.474×10^{-9}, respectively.

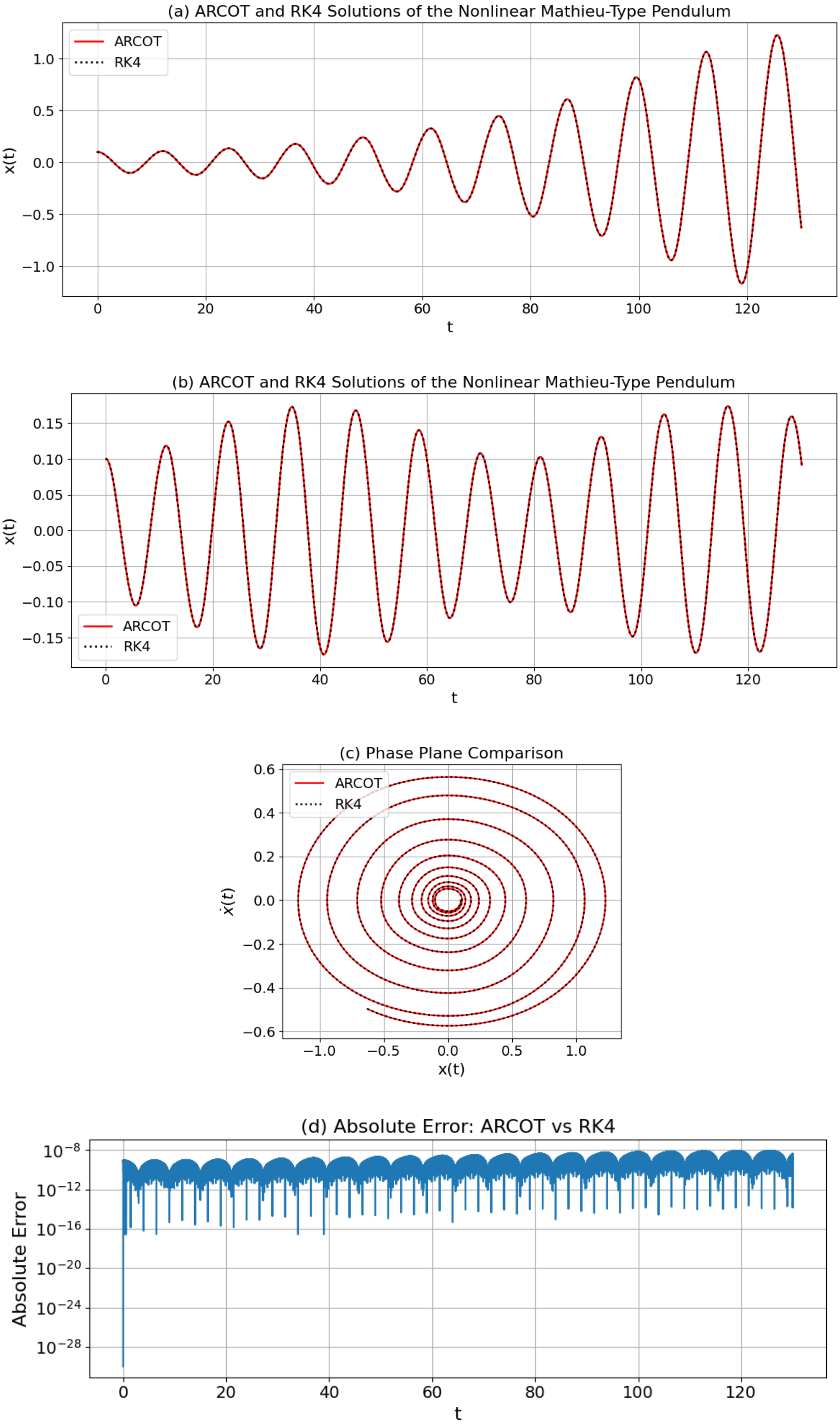

Figure 5. (**a**) Comparison of ARCOT and RK4 displacement responses for the nonlinear Mathieu-type pendulum in the unstable regime ($\delta = 0.25$). (**b**) Comparison of ARCOT and RK4 displacement responses for the nonlinear Mathieu-type pendulum in the stable regime ($\delta = 0.30$). (**c**) Phase-plane comparison of ARCOT and RK4 for the nonlinear Mathieu-type pendulum in the unstable regime $\delta = 0.25$. (**d**) Absolute error of the ARCOT solution relative to the RK4 reference solution for the nonlinear Mathieu-type pendulum in the unstable regime $\delta = 0.25$.

4.5. Cubic–Quintic Double-Well Duffing Oscillator

In this example, the proposed ARCOT method is applied to a forced damped cubic–quintic Duffing oscillator possessing a double-well potential structure. Due to the simultaneous presence of damping, external forcing, cubic nonlinearity, and quintic stiffness effects, the system exhibits strongly nonlinear oscillatory behavior and constitutes a challenging benchmark problem for adaptive high-order numerical methods.

Example 5. *The governing equation given by [23] is*

$$m\ddot{x}(t) + c\dot{x}(t) + kx(t) + \alpha x^3(t) + \beta x^5(t) = F_0\cos(\omega t)$$

subject to the initial conditions

$$x(0) = 1,\ \ \dot{x}(0) = 0$$

In line with [23], the system parameters are selected as

$$m = 1, c = 0.2, k = -1, \alpha = 1, \beta = 0.1, F_0 = 0.3, \omega = 1.2$$

Since the linear stiffness coefficient is negative $(k < 0)$ while the higher-order nonlinear stiffness coefficients are positive $(\alpha > 0, \beta > 0)$, the corresponding potential energy function possesses a double-well structure. Consequently, the system contains two stable potential minima separated by an unstable equilibrium region near the origin. Such systems are known to exhibit rich nonlinear dynamics including bistability, large-amplitude oscillations, interwell transitions, and strong sensitivity to external excitation.

The equation is solved using the proposed ARCOT framework and compared with the classical RK45 solution. The obtained displacement responses demonstrate excellent agreement between the two methods throughout the considered interval, confirming the accuracy and robustness of the residual-controlled overlapping continuation strategy.

For this example, the ARCOT computation employed $N = 30$, $\varepsilon = 10^{-2}$, and $\theta = 15/29 \approx 0.5172$. 30 uniformly spaced continuation points were used within each full Taylor interval, while the residual was evaluated at 100 uniformly spaced points over the accepted interval. The initial interval length was $H_0 = 0.25$, with $H_{\min} = 10^{-6}$ and $H_{\max} = 0.50$.

ARCOT completed the solution with 237 accepted intervals and no rejected intervals, with maximum and mean residuals of 5.690×10^{-15} and 1.315×10^{-15}, respectively. The computational times were approximately 6.08 s for ARCOT and 0.90 s for RK45. RK45 required 1843 internal accepted points and 11,090 function evaluations. The maximum and mean absolute differences between the ARCOT and RK45 solutions were 2.345×10^{-5} and 3.196×10^{-6}, respectively.

As shown in Figure 6a–c, the ARCOT and RK45 displacement responses exhibit close agreement throughout the integration interval (Figure 6a). The corresponding phase-plane trajectories are also nearly coincident (Figure 6b), demonstrating that ARCOT accurately captures the strongly nonlinear oscillatory dynamics of the forced damped cubic–quintic double-well Duffing oscillator. The absolute error of ARCOT relative to the RK45 reference solution remains small throughout the simulation (Figure 6c), further confirming the numerical agreement between the two methods. These results demonstrate that ARCOT successfully captures the complex dynamics associated with the double-well system while maintaining stable numerical behavior over the considered integration interval.

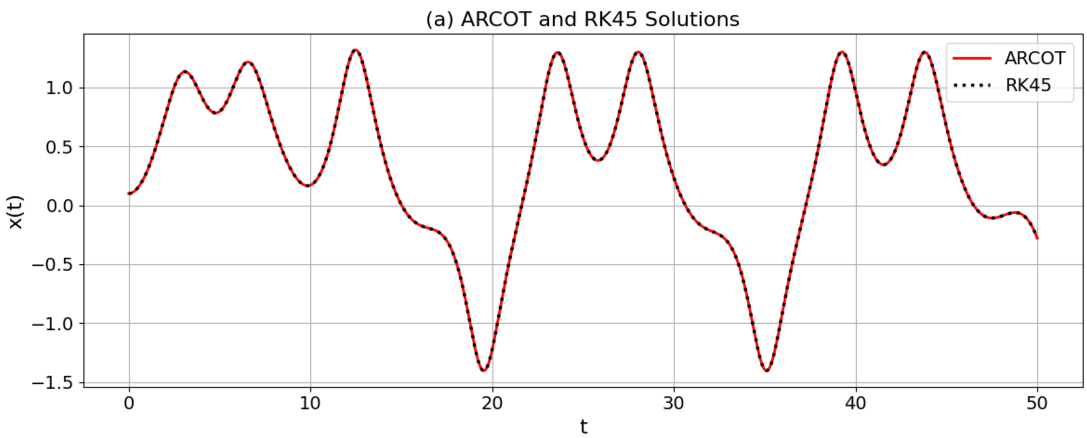

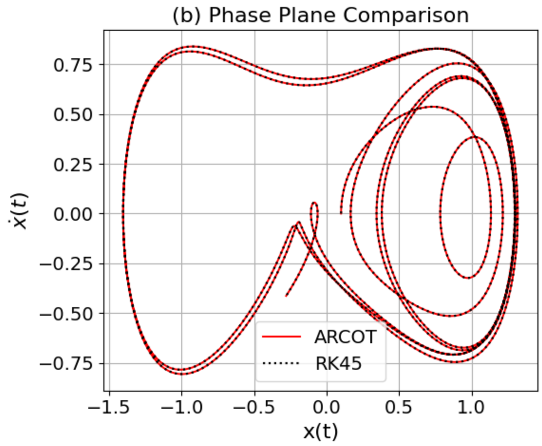

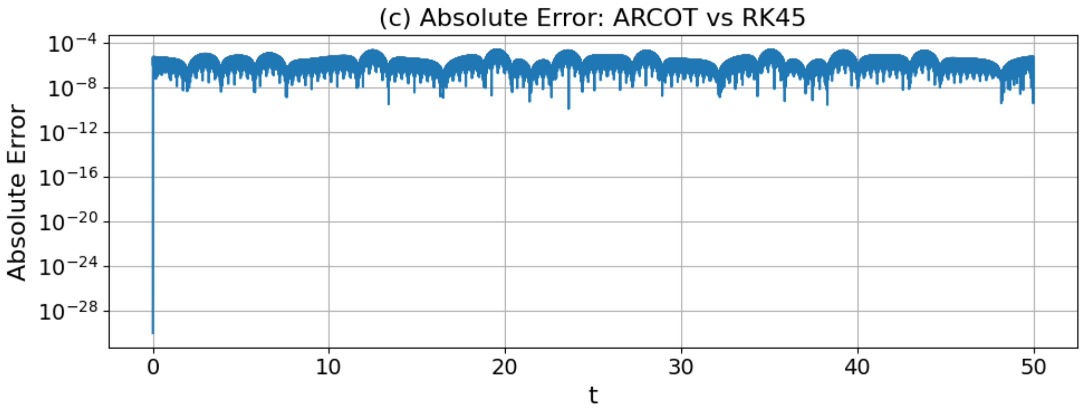

Figure 6. (**a**) Comparison of ARCOT and RK45 displacement responses for the forced damped cubic–quintic double-well Duffing oscillator. (**b**) Phase-plane comparison of ARCOT and RK45 for the forced damped cubic–quintic double-well Duffing oscillator. (**c**) Absolute error of the ARCOT solution relative to the RK45 reference solution for the forced damped cubic–quintic double-well Duffing oscillator.

5. Comparative Analysis and Discussion

The numerical results demonstrate that ARCOT provides accurate and stable solutions for the nonlinear oscillators considered in this study. Its methodological distinction lies in the combined use of high-order Taylor recurrence, overlapping continuation, residual-based acceptance/rejection, and adaptive interval regulation. These mechanisms operate within a unified continuation framework and distinguish ARCOT from conventional Taylor, Runge–Kutta, and residual-based approaches.

5.1. Comparison with Runge–Kutta Methods

The ARCOT solutions show close agreement with the RK4 and RK45 reference solutions in terms of displacement responses, phase-plane trajectories, and absolute differences. The computational comparisons reported for the individual examples also show that RK4 and RK45 are faster than the present ARCOT implementation. ARCOT should therefore not be interpreted as providing a general computational-speed advantage over Runge–Kutta methods. Its contribution instead concerns the manner in which local approximation quality and continuation are controlled.

Classical fixed-step RK4 advances the solution through successive predetermined steps, whereas adaptive RK45 regulates the step size using an embedded local-error estimate. ARCOT employs a different adaptive principle: a high-order Taylor approximation is constructed over a candidate interval, and the residual of the original governing equation is evaluated directly over the accepted portion. The interval is accepted only when the prescribed residual criterion is satisfied. Thus, ARCOT provides direct residual monitoring in addition to adaptive continuation.

The computational cost of this strategy is higher because ARCOT requires high-order coefficient generation and residual evaluation at multiple points within each continuation interval. Nevertheless, the reported accepted/rejected intervals, computational times, RK45 function evaluations, and solution differences demonstrate that ARCOT maintains close agreement with established Runge–Kutta reference solutions across the investigated nonlinear regimes.

5.2. Comparison with Taylor- and Residual-Based Methods

ARCOT is related to classical Taylor methods and Taylor-based collocation and splitting approaches [27,30–32,34,38]. However, its novelty does not arise from Taylor expansion alone. In conventional Taylor continuation, the solution is generally propagated between successive interval endpoints. ARCOT instead advances from an interior continuation point, producing overlapping local Taylor intervals. This reduces reliance on terminal regions of a local expansion, where truncation deterioration may become more pronounced.

Residual evaluation itself is also established in methods such as FRPSM [49], ARPSM [50], ARA-residual approaches [26], and other residual-based formulations [28]. The distinguishing feature of ARCOT is that the residual is incorporated directly into the adaptive continuation procedure. It determines whether a candidate interval is accepted or rejected and influences the subsequent continuation length. Accordingly, the methodological contribution of ARCOT is the integration of overlapping Taylor continuation and residual-driven adaptive interval control, rather than any one of these components considered independently.

This distinction is particularly relevant to the Taylor-Splitting Collocation Method [38]. Although both methods employ Taylor representations together with interval decomposition, ARCOT additionally combines interior overlapping continuation with direct residual-based acceptance and adaptive interval regulation. This unified mechanism constitutes the principal difference from existing Taylor-based formulations.

5.3. Stability and Convergence Considerations

The stability characteristics observed in the numerical examples can be attributed primarily to the interaction between overlapping continuation and residual control. Advancing from an interior point of the current Taylor interval reduces dependence on its terminal region and thereby limits the propagation of local approximation deterioration into subsequent intervals. Residual monitoring provides an additional safeguard: if the governing-equation residual exceeds the prescribed tolerance, the candidate interval is rejected and recomputed using a reduced continuation length. In smoother regions, the interval may be enlarged within the prescribed bounds.

The numerical experiments show that the residual remained below the prescribed tolerance for the accepted intervals and that ARCOT remained in close agreement with RK4, RK45, and, where available, the Jacobi elliptic solution. These observations provide numerical evidence of stable and convergent behavior for the problems considered.

However, these numerical results should not be interpreted as a general analytical convergence proof. The present framework provides numerical convergence control through high-order local approximation, residual monitoring, interval rejection, and adaptive continuation. Establishing rigorous global convergence and stability bounds for general nonlinear systems remains an important subject for future theoretical investigation.

5.4. Limitations and Future Work

The principal limitation of the current ARCOT implementation is computational cost. High-order Taylor coefficient generation and repeated residual evaluation can become expensive for strongly nonlinear, high-dimensional, or coupled systems. The method is also primarily formulated for sufficiently smooth problems; discontinuities, impacts, and switching dynamics may require additional treatment. Furthermore, computational performance depends on the Taylor order, residual tolerance, overlap parameter, and allowable continuation lengths.

Despite these limitations, the numerical results indicate that the combination of residual-controlled adaptivity and overlapping high-order Taylor continuation provides a robust framework for nonlinear oscillatory systems. Future work should therefore focus on rigorous convergence analysis, more efficient coefficient-generation algorithms, automatic parameter selection, and extensions to coupled, fractional, delay, and distributed dynamical systems.

6. Conclusions

In this study, a new adaptive high-order continuation framework, the ARCOT method, was proposed for the numerical solution of strongly nonlinear oscillatory systems. The method combines local high-order Taylor expansion, overlapping continuation intervals, residual-controlled adaptivity, and adaptive continuation interval regulation within a unified computational framework.

The proposed methodology was successfully applied to several important nonlinear dynamical systems, including Duffing, cubic–quintic, Van der Pol, Mathieu-type, and double-well oscillators. Comparisons with RK4, RK45, Taylor-based methods, and analytical or semi-analytical solutions available in the literature demonstrated excellent agreement and confirmed the reliability of the proposed approach.

The obtained results showed that overlapping continuation significantly improves long-time numerical stability by reducing cumulative continuation errors between neighboring intervals. The residual-monitoring strategy effectively prevents divergence by continuously evaluating the governing equation residual throughout the continuation process, while adaptive interval regulation automatically adjusts local continuation lengths according to the nonlinear complexity of the response. The numerical experiments further demonstrated that ARCOT accurately captures strongly nonlinear behaviors including nonlinear resonance, parametric instability, relaxation-type oscillations, and double-well dynamics without noticeable numerical drift.

Compared with conventional Taylor continuation approaches, ARCOT introduces an additional stabilization mechanism through residual-controlled overlapping continuation, which constitutes one of the principal methodological contributions of the present study. Overall, the results indicate that ARCOT provides a robust, accurate, and flexible framework for nonlinear oscillatory systems and represents a promising alternative to conventional fixed-step and adaptive integration schemes.

The present work focused on nonlinear single-degree-of-freedom systems; however, the ARCOT framework possesses considerable extension potential. Future studies may consider fractional and delay differential equations, chaotic oscillators, and coupled multi-degree-of-freedom systems. Extensions toward nonlinear partial differential equations, particularly beam vibrations and distributed wave problems, also appear promising. In addition, hybrid ARCOT–PINN formulations may provide an effective direction for combining residual-controlled continuation with physics-informed machine learning frameworks. These extensions may further establish ARCOT as a general adaptive computational methodology for nonlinear dynamical systems.

Author Contributions

M.Ç.: Conceptualization, Writing-original draft, Software, Investigation; S.S.: Visualization, Validation; N.B.S.: Writing-review & editing. All authors have read and agreed to the published version of the manuscript.

Funding

This research received no external funding.

Data Availability Statement

The datasets generated and analyzed during the current study are available from the corresponding author on reasonable request.

Conflicts of Interest

The authors declare no conflict of interest.

Use of AI and AI-Assisted Technologies

During the preparation of this work, the authors used chatGPT for language revision and improvement of readability and clarity. After using this tool, the authors reviewed and edited the content as needed and take full responsibility for the content of the published article.

References

1. Samaniego, E.; Anitescu, C.; Goswami, S.; et al. An Energy Approach to the Solution of Partial Differential Equations in Computational Mechanics via Machine Learning: Concepts, Implementation and Applications. *Comput. Methods Appl. Mech. Eng.* **2020**, *362*, 112790. https://doi.org/10.1016/j.cma.2019.112790.
2. Bulut, S.; Yiğider, M. Deep Learning Approaches for β-Conformable Fractional Differential Equations: A PINN, NRPINN-S, and NRPINN-Un Based Solutions. *AIMS Math.* **2025**, *10*, 13721–13740. https://doi.org/10.3934/math.2025618.
3. Ali, A.; Senu, N.; Wahi, N.; et al. An Adaptive Algorithm for Numerically Solving Fractional Partial Differential Equations Using Hermite Wavelet Artificial Neural Networks. *Commun. Nonlinear Sci. Numer. Simul.* **2024**, *137*, 108121. https://doi.org/10.1016/j.cnsns.2024.108121.
4. Abdellatif, B.; Benazouz, C.; Ahmed, M.B. Dynamic Response Estimation of an Equivalent Single Degree of Freedom System Using Artificial Neural Network and Nonlinear Static Procedure. *Res. Eng. Struct. Mater.* **2024**, *10*, 431–444. https://doi.org/10.17515/resm2023.40me0818rs.

5. Kim, J. Extended Framework of Hamilton's Principle for Single-Degree-of-Freedom Nonlinear Damping Systems. *J. Low Freq. Noise Vib. Act. Control.* **2021**, *40*, 1437–1452. https://doi.org/10.1177/1461348420961611.
6. Chen, M.; Li, S.; Cui, H. Longitudinal Dynamic Behavior Study of a Vibrating Rod Connected through an Elastic Nonlinear Single Degree Freedom Coupler. *Sci. Rep.* **2024**, *14*, 27326. https://doi.org/10.1038/s41598-024-78762-z.
7. Bayat, M.; Pakar, I. On the Approximate Analytical Solution to Non-Linear Oscillation Systems. *Shock Vib.* **2013**, *20*, 43–52. https://doi.org/10.3233/sav-2012-0726.
8. Boone, E.; Hannig, J.; Ghanam, R.; et al. Model Validation of a Single Degree-of-Freedom Oscillator: A Case Study. *Stats* **2022**, *5*, 1195–1211. https://doi.org/10.3390/stats5040071.
9. Witkowski, K.; Kudra, G.; Wasilewski, G.; et al. Mathematical Modelling, Numerical and Experimental Analysis of One-Degree-of-Freedom Oscillator with Duffing-Type Stiffness. *Int. J. Non-Linear Mech.* **2022**, *138*, 103859. https://doi.org/10.1016/j.ijnonlinmec.2021.103859.
10. Fujii, K.; Kanno, H.; Nishida, T. Formulation of the Time-Varying Function of Momentary Energy Input to a Single-Degree-of-Freedom System Using Fourier Series. *J. Jpn. Assoc. Earthq. Eng.* **2021**, *21*, 3_28–3_47. https://doi.org/10.5610/jaee.21.3_28.
11. Salsa Junior, R.G. Forced Vibration of Systems with One Degree of Freedom. In *Fundamentals of the Theory of Mechanical Vibrations*; Springer: Cham, Switzerland, 2025; pp. 95–144. https://doi.org/10.1007/978-3-031-83995-5_3.
12. Newaz, A.A.H.; Mitra, R.; Jahan, R.; et al. Free Vibration Characteristics of Single-Degree-of-Freedom (SDOF) Mechanical Systems: Investigating through Theory, Experimentation and Numerical Simulation. In *Engineering Research: Perspectives on Recent Advances*; BP International: West Bengal, India, 2025; Vol. 7, pp. 43–57. https://doi.org/10.9734/bpi/erpra/v7/5456.
13. McIntosh, R.; Dubay, R.; Garland, P. A Solution to the Response of a Single Degree of Freedom System to Swept Sine Inputs. In Proceedings of the 2025 IEEE International Systems Conference (SysCon), Montreal, QC, Canada, 7–10 April 2025; pp. 1–8. https://doi.org/10.1109/syscon64521.2025.11014862.
14. Kojima, K.; Takewaki, I. Critical Response of a Single-Degree-of-Freedom System with Bilinear Hysteresis and Viscous Damping under Triple Impulse. *Front. Built Environ.* **2025**, *11*, 1539299. https://doi.org/10.3389/fbuil.2025.1539299.
15. Neal, H.L.; Nayfeh, A.H. Response of a Single-Degree-of-Freedom System to a Non-Stationary Principal Parametric Excitation. *Int. J. Non-Linear Mech.* **1990**, *25*, 275–284. https://doi.org/10.1016/0020-7462(90)90057-g.
16. Mehdipour, I.; Ganji, D.D.; Mozaffari, M. Application of the Energy Balance Method to Nonlinear Vibrating Equations. *Curr. Appl. Phys.* **2010**, *10*, 104–112. https://doi.org/10.1016/j.cap.2009.05.016.
17. Zavodney, L.D.; Nayfeh, A.H.; Sanchez, N.E. Bifurcations and Chaos in Parametrically Excited Single-Degree-of-Freedom Systems. *Nonlinear Dyn.* **1990**, *1*, 1–21. https://doi.org/10.1007/bf01857582.
18. Alevras, P.; Yurchenko, D. Stochastic Rotational Response of a Parametric Pendulum Coupled with an SDOF System. *Probab. Eng. Mech.* **2014**, *37*, 124–131. https://doi.org/10.1016/j.probengmech.2013.10.008.
19. Kural, S. Effect of Spring Mid-Support Condition on the Vibrations of the Axially Moving String. *Int. Adv. Res. Eng. J.* **2020**, *4*, 191–199. https://doi.org/10.35860/iarej.757503.
20. Beléndez, A.; Beléndez, T.; Martínez, F.J.; et al. Exact Solution for the Unforced Duffing Oscillator with Cubic and Quintic Nonlinearities. *Nonlinear Dyn.* **2016**, *86*, 1687–1700. https://doi.org/10.1007/s11071-016-2986-8.
21. Vakakis, A.F.; Blanchard, A. Exact Steady States of the Periodically Forced and Damped Duffing Oscillator. *J. Sound Vib.* **2018**, *413*, 57–65. https://doi.org/10.1016/j.jsv.2017.10.030.
22. Moatimid, G.M.; Amer, T.S. Dynamical System of a Time-Delayed ϕ6-Van Der Pol Oscillator: A Non-Perturbative Approach. *Sci. Rep.* **2023**, *13*, 11942. https://doi.org/10.1038/s41598-023-38679-5.
23. Salas, A.H.; Albalawi, W.; El-Tantawy, S.A.; et al. Some Novel Approaches for Analyzing the Unforced and Forced Duffing–Van Der Pol Oscillators. *J. Math.* **2022**, *2022*, 2174192. https://doi.org/10.1155/2022/2174192.
24. Motonaga, S. Subharmonic Melnikov Functions and Nonintegrability for Autonomous and Non-Autonomous Perturbations of Single-Degree-of-Freedom Hamiltonian Systems near Periodic Orbits. *Phys. D Nonlinear Phenom.* **2024**, *460*, 134088. https://doi.org/10.1016/j.physd.2024.134088.
25. Yıldız, B.; Sınır, S.M.; Sınır, B.G.L. A General Solution Procedure for Nonlinear Single Degree of Freedom Systems Including Fractional Derivatives. *Int. J. Non-Linear Mech.* **2025**, *169*, 104966. https://doi.org/10.1016/j.ijnonlinmec.2024.104966.
26. Burqan, A.; Saadeh, R.; Qazza, A.; et al. ARA-Residual Power Series Method for Solving Partial Fractional Differential Equations. *Alex. Eng. J.* **2023**, *62*, 47–62. https://doi.org/10.1016/j.aej.2022.07.022.
27. Sezer, M.; Yalçinbaş, S.; Gülsu, M. A Taylor Polynomial Approach for Solving Generalized Pantograph Equations with Nonhomogeneous Term. *Int. J. Comput. Math.* **2008**, *85*, 1055–1063. https://doi.org/10.1080/00207160701466784.
28. Bahşı, M.M.; Çevik, M.; Sezer, M. Orthoexponential Polynomial Solutions of Delay Pantograph Differential Equations with Residual Error Estimation. *Appl. Math. Comput.* **2015**, *271*, 11–21. https://doi.org/10.1016/j.amc.2015.08.101.
29. Çevik, M.; Bahşı, M.M.; Sezer, M. Solution of the Delayed Single Degree of Freedom System Equation by Exponential Matrix Method. *Appl. Math. Comput.* **2014**, *242*, 444–453. https://doi.org/10.1016/j.amc.2014.05.111.

30. Gülsu, M.; Sezer, M. The Approximate Solution of High-Order Linear Difference Equations with Variable Coefficients in Terms of Taylor Polynomials. *Appl. Math. Comput.* **2005**, *168*, 76–88. https://doi.org/10.1016/j.amc.2004.08.043.
31. Gülsu, M.; Sezer, M. A Taylor Polynomial Approach for Solving Differential-Difference Equations. *J. Comput. Appl. Math.* **2006**, *186*, 349–364. https://doi.org/10.1016/j.cam.2005.02.009.
32. Kurt, N.; Çevik, M. Polynomial Solution of the Single Degree of Freedom System by Taylor Matrix Method. *Mech. Res. Commun.* **2008**, *35*, 530–536. https://doi.org/10.1016/j.mechrescom.2008.05.001.
33. Çevik, M. Application of Taylor Matrix Method to the Solution of Longitudinal Vibration of Rods. *Math. Comput. Appl.* **2010**, *15*, 334–343. https://doi.org/10.3390/mca15030334.
34. Bahşı, M.M.; Çevik, M. Taylor Matrix Solution of the Mathematical Model of the RLC Circuits. *Math. Comput. Appl.* **2013**, *18*, 467–475. https://doi.org/10.3390/mca18030467.
35. Savaşaneril, N.B. Lucas Polynomial Solution of the Single Degree of Freedom System. *Sci. Res. Commun.* **2023**, *3*, 1–10. https://doi.org/10.52460/src.2023.002.
36. Yüzbaşı, Ş.; Çetin, B. A Boubaker Collocation Method to Solve the Single Degree of Freedom System. In *Analysis, Approximation, Optimization: Computation and Applications: In Honor of Gradimir V. Milovanović on the Occasion of His 75th Birthday*; Springer Optimization and Its Applications; Stanić, M.P., Albijanić, M., Djurčić, D., et al., eds.; Springer: Cham, Switzerland, 2025; Vol. 224, pp. 415–424. https://doi.org/10.1007/978-3-031-85743-0_21.
37. Çevik, M.; Savaşaneril, N.B.; Sezer, M. A Review of Polynomial Matrix Collocation Methods in Engineering and Scientific Applications. *Arch. Comput. Methods Eng.* **2025**, *32*, 3355–3373. https://doi.org/10.1007/s11831-025-10235-6.
38. Çayan, S.; Özhan, B.B.; Sezer, M. A Taylor-Splitting Collocation Approach and Applications to Linear and Nonlinear Engineering Models. *Chaos Solitons Fractals* **2022**, *164*, 112683. https://doi.org/10.1016/j.chaos.2022.112683.
39. Aghazadeh, N.; Mohammadi, A.; Tanoglu, G. Taylor Wavelets Collocation Technique for Solving Fractional Nonlinear Singular PDEs. *Math. Sci.* **2024**, *18*, 41–54. https://doi.org/10.1007/s40096-022-00483-z.
40. Al-Nana, A.A.; Alomari, M.W.; Batiha, I.M. The Modified Taylor Method for Approximating Solutions of Initial Value Problems. *Int. Rev. Model. Simul. (IREMOS)* **2024**, *17*, 338–347. https://doi.org/10.15866/iremos.v17i5.25176.
41. Pakdemirli, M. On a New Two-Point Taylor Expansion with Applications. *Qeios* **2024**, *6*. https://doi.org/10.32388/dfkj12.2.
42. Boscarino, S.; Macca, E. Adaptive Time-Step Semi-Implicit One-Step Taylor Scheme for Stiff Ordinary Differential Equations. In Proceedings of the Computational Mechanics and Applied Mathematics: Perspectives from Young Scholars (GIMC SIMAI Young 2024), Naples, Italy, 10–12 July 2024; Marmo, F., Cuomo, S., Cutolo, A., eds.; Springer: Cham, Switzerland, 2025; pp. 223–235. https://doi.org/10.1007/978-3-031-76591-9_21.
43. Taylor, J.M.; Bastidas, M.; Calo, V.M.; et al. Adaptive Deep Fourier Residual Method via Overlapping Domain Decomposition. *Comput. Methods Appl. Mech. Eng.* **2024**, *427*, 116997. https://doi.org/10.1016/j.cma.2024.116997.
44. Liu, W.; Liu, Y. A Forward Progressive Physics Informed Neural Network with Taylor Series Expansion for Solving Evolution Partial Differential Equations. *AIMS Math.* **2025**, *10*, 24857–24900. https://doi.org/10.3934/math.20251101.
45. Le Guisquet, S.; Amabili, M. Identification by Means of a Genetic Algorithm of Nonlinear Damping and Stiffness of Continuous Structures Subjected to Large-Amplitude Vibrations. Part I: Single-Degree-of-Freedom Responses. *Mech. Syst. Signal Process.* **2021**, *153*, 107470. https://doi.org/10.1016/j.ymssp.2020.107470.
46. Salas, A.H.; Martínez H, L.J.; Ocampo R, D.L. Analytical Solution for the Cubic-Quintic Duffing Oscillator Equation with Physics Applications. *Complexity* **2022**, *2022*, 9269957. https://doi.org/10.1155/2022/9269957.
47. Alim, M.A.; Kawser, M.A. Illustration of the Homotopy Perturbation Method to the Modified Nonlinear Single Degree of Freedom System. *Chaos Solitons Fractals* **2023**, *171*, 113481. https://doi.org/10.1016/j.chaos.2023.113481.
48. Kovacic, I.; Rand, R.; Mohamed Sah, S. Mathieu's Equation and Its Generalizations: Overview of Stability Charts and Their Features. *Appl. Mech. Rev.* **2018**, *70*, 020802. https://doi.org/10.1115/1.4039144.
49. Khalouta, A.; Kadem, A. A New Computational for Approximate Analytical Solutions of Nonlinear Time-Fractional Wave-like Equations with Variable Coefficients. *AIMS Math.* **2020**, *5*, 1–14. https://doi.org/10.3934/math.2020001.
50. Liaqat, M.I.; Etemad, S.; Rezapour, S.; et al. A Novel Analytical Aboodh Residual Power Series Method for Solving Linear and Nonlinear Time-Fractional Partial Differential Equations with Variable Coefficients. *AIMS Math.* **2022**, *7*, 16917–16948. https://doi.org/10.3934/math.2022929.